Electron Transfer in a Flexible, Tethered Donor−Acceptor Pair: The Influence of Solute Conformation on Solvent-Dependent Free Energies

John F. Kauffman,* Mazdak Khajehpour, and Na'il Saleh

Department of Chemistry, University of Missouri−Columbia, Columbia, Missouri 65211

Received: June 23, 2003; In Final Form: February 15, 2004

ADMA (1-(9-anthryl)-3-(4-dimethylanilino)propane) undergoes charge transfer following excitation of the anthryl moiety and forms an exciplex. Two mechanisms of charge transfer have been identified in previous work, and the operative mechanism depends on the polarity of the solvent. These are referred to as the nonpolar and the polar mechanisms. In polar solvents the charge transfer is rapid and occurs in an extended conformation followed by folding to form the exciplex. In hydrocarbons the exciplex formation rate is much slower and requires the donor and acceptor moieties to attain the correct geometry prior to charge transfer. Prior to the present work, it has been assumed that the charge transfer mechanism in hydrocarbons is diffusion controlled. In this work we demonstrate that charge transfer in nonpolar solvents is an activated process. We measure the rate of charge transfer in ethers (solvents of modest polarity with $\epsilon = 3-4.3$) and compare these to charge transfer rates in alkanes having similar viscosity. Whereas alkane charge transfer rates are well correlated to a viscosity power law, the rates in ethers are accelerated. We calculate the solvent-dependent driving force for the reaction using two different models, and the results also allow us to calculate the reaction reorganization energies. These are then used to estimate the activation barrier for the reaction, which demonstrate that the reaction is not encounter controlled. Analysis of the results demonstrates that solvent stabilization of the product state accelerates the charge transfer rate, in accord with Marcus theory, for solvents with dielectric constants between 2 and ∼4. Solvents with dielectric constants between 4 and 5 exhibit additional acceleration of the charge transfer reaction due to solvent dependence of the distance at which charge transfer occurs. This reflects a transition between the nonpolar and polar mechanisms.

I. Introduction

Molecules in the excited state are much more reactive than in the ground state. The charge donating and accepting ability of a molecule increases when the molecule is in its excited state, enabling some molecules, especially aromatic hydrocarbons, to form charge transfer complexes.[1] The exciplex that forms between electronically excited anthracene and ground state dimethylaniline has been particularly well studied.[2] When the donor and acceptor groups are tethered together by an alkane chain, the efficiency of the charge transfer process becomes subject to geometric constraints and is also influenced by solvent polarity.[3−9] Mataga and co-workers demonstrated that joining the anthracene and dimethylaniline moieties by a propyl chain (1-(9-anthryl)-3-(4-dimethylanilino)propane, hereafter abbreviated to ADMA; see Figure 1) minimizes the geometric constraints for charge transfer, allowing excited state charge transfer to occur in a broad range of solvents and in the gas phase. The photochemical relaxation mechanism of ADMA follows the scheme given in Figure 2.[7,10−14] The locally excited (LE) state of the molecule is prepared by absorption of a 387 nm photon, which selectively excites the anthryl moiety. The emissive exciplex has a folded geometry and is described in the literature as the sandwich heteroexcimer (SH). In nonpolar solvents (solvents with dielectric constant, ϵ, less than 5) the locally excited state of ADMA must obtain the correct geometry (assumed to be similar to the geometry of the emissive exciplex) in order for charge transfer to occur. Experimentally, the decay of the LE emission of ADMA in nonpolar solvents is observed to be monoexponential and is consistent with kinetic analysis of the nonpolar mechanism shown in Figure 2, in which charge transfer quenches the LE emission. Polar solvents can mediate charge transfer through the rapid formation of an extended charge transfer complex, described in the literature as the loose heteroexcimer (LH), which then collapses into the stable SH conformation. Kinetic analysis of the polar mechanism in Figure 2 predicts a biexponential decay of the LE emission, and the biexponential decay is observed experimentally when the solvent dielectric constant exceeds a value of 5.[15]

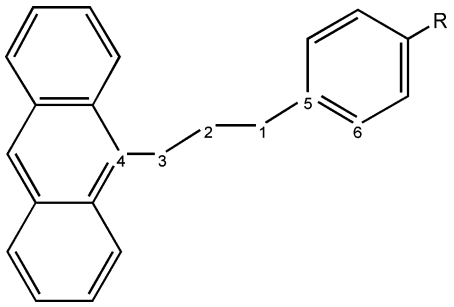

Figure 1. Structure of ADMA (R = $N(CH_3)_2$) and APP (R = H). See Figure 2 for representative structures.

Studies performed on the intermolecular anthracene−dimethylaniline exciplex have demonstrated that the formation rate is diffusion controlled.[2] This result is in agreement with the conventional knowledge of charge transfer and exciplex formation.[16] Face to face exciplexes between planar aromatic com-

* To whom correspondence should be addressed. E-mail: kauffmanj@missouri.edu.

10.1021/jp035784s CCC: $27.50
Published on Web 03/26/2004

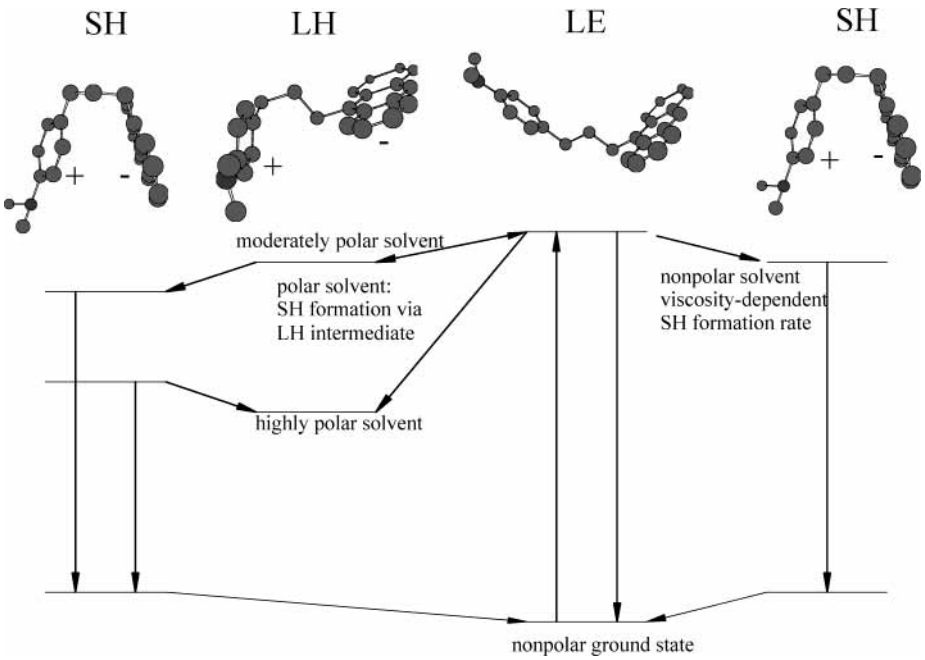

Figure 2. Energy level scheme that governs excited state isomerization kinetics of ADMA. The scheme demonstrates that sandwich heteroexcimer (SH) state formation is mediated by both solvent viscosity and solvent polarity. In polar solvents the favored pathway to the SH state is through the charge-separated loose heteroexcimer (LH) intermediate. The nonemissive LH state becomes the low-energy configuration in highly polar solvents.

pounds have a high degree of electronic coupling.[16] Ando[17] has performed a detailed theoretical study of the dynamics of the bimolecular electron transfer reaction of anthracene with dimethylaniline in acetonitrile. The study demonstrates that the potential energy surfaces for this reaction are well represented by parabolas in the curve crossing region, and that in acetonitrile the reaction is in the Marcus normal regime at distances longer than 4 Å. Evaluation of the electronic coupling reveals ~300 cm^{-1} coupling at a distance of 7 Å, increasing to ~700 cm^{-1} at 5 Å. The distance-dependent transmission coefficient parameter in an interpolation formula between adiabatic and nonadiabatic regimes has a value of 1 for distances of 7 Å or less, indicating that the reaction is adiabatic according to this investigation. Ando[17] also notes that turning off the solvent charges reduces the overlap integral between initial and final states at the potential crossing point by ~35%. Furthermore, the overlap integral has an orientational variance that is nearly equal to its mean value when computed over 20 configurations at both 5 and 7 Å. But though both solvent polarity and relative reactant orientation mediate electronic coupling, the reactants are capable of sampling orientational configurations such that adiabatic charge transfer occurs, even in nonpolar solvents.

With respect to intramolecular systems, Waldeck, Zimmt, and co-workers[18,19] have reported solvent-mediated electronic coupling in donor−bridge−acceptor molecules with rigid bridges that change by as much as a factor of 3 with solvent. In vacuo electronic coupling between two systems that differ only in the geometry of donor and acceptor indicates that the face-to-face donor acceptor geometry, such as that of the ADMA-folded conformation, result in a coupling that is ~70% larger than the extended geometry. This case highlights the sensitivity of electronic coupling to donor−acceptor geometry, even in the absence of solvent effects.

The results described above suggest that the ADMA intramolecular exciplex formation rate will be diffusion controlled in low-polarity solvents, with bimolecular diffusion replaced by intramolecular diffusion characterized by the relaxation time of the propyl chain that tethers the reactants. In fact, Wang et al.[8] have measured the exciplex formation rate in some alkanes and have obtained a power law correlation between the viscosity and the exciplex formation rate. Though dependence of the charge transfer rate on viscosity is expected for diffusion controlled reactions, the quenching rates reported by Wang et al. are smaller than the chain relaxation times of analogous alkane chains such as pentane. This observation led Wang et al. to postulate that the observed quenching times result from unexpectedly strong solvent viscous drag on the aromatic moieties that prevents the donor and acceptor from freely diffusing toward each other. Though this postulate offers a plausible explanation for the slow rate of ADMA exciplex formation in nonpolar solvents, we will present evidence that indicates that the exciplex formation reaction is not diffusion controlled, owing to a modest barrier to charge transfer, even in the folded configuration.

In the bimolecular reaction of anthracene and dimethylaniline, the approach of the donor and acceptor moieties toward each other is unhindered, favoring reaction over diffusion away from one another. On the other hand, the approach of the tethered reactants toward one another is governed by the chain conformational restrictions. Furthermore, the tethered reactants experience a driving force that opposes the formation of the folded form of the locally excited state. Itoh and co-workers[20,21] have quantified the relative stability of various conformations of analogues of ADMA on the basis of supersonic jet spectra and semiempirical calculations. They report that a partially folded configuration is at least 7 kJ/mol less stable than the extended form of the ground state, whereas the barrier to unfolding is in the range of 1 kJ/mol. These observations suggest that charge transfer quenching of the locally excited state emission should depend on the relative rates of the unfolding and electron transfer reactions in addition to the rate of diffusion of reactants toward one another.

To investigate this alternative description of the charge transfer process between tethered reactants, we have measured the rate of quenching of the ADMA locally excited state emission in several solvents of low polarity ($\epsilon < 5$). By

comparing solvents of varying dielectric constant with hydrocarbon solvents of similar viscosity, we are able to separate solvent dielectric and viscous influences on the rate of the charge transfer reaction. We observe an acceleration of the charge transfer rate when the solvent dielectric constant increases at fixed viscosity. This observation provides evidence that the rate of the intramolecular charge transfer reaction is not diffusion controlled in hydrocarbon solvents and indicates the existence of a modest barrier to charge transfer, even in the folded configuration of the locally excited state. Activated, photoinitiated electron transfer is well-described by Marcus theory,[22−29] and we therefore anticipate that the barrier to electron transfer should be related to the solvent stabilization of the exciplex.

This paper is organized into six sections. Section II describes the experimental and computational methods used, and section III presents the experimentally measured rates of electron transfer in ethers, solvents of modest polarity, in comparison with ADMA charge transfer rates in alkanes. In section IV we develop a kinetic scheme that postulates an intermediate folded configuration of the locally excited state of the molecule, which can either unfold or undergo electron transfers. Section V describes the application of the Rehm−Weller[22] expression to the calculation of the thermodynamic driving force for the ADMA charge transfer reaction in both folded and extended configurations. This section includes calculation of the steric energy, Coulomb energy, and ion solvation energies, which are necessary for the application of the Rehm−Weller model. Section VI presents a three state potential energy picture that is used to develop a simple expression for the thermodynamic driving force for the ADMA charge transfer reaction in the folded configuration on the basis of charge transfer state emission spectra. This model also utilizes the reorganization energy of the reaction. By comparing the driving force calculated by this model to the Rehm−Weller result in acetonitrile, we are able to estimate the total reorganization energy for the reaction in this solvent. We then utilize a continuum model for solvent reorganization to calculate the total reorganization energy and the thermodynamic driving force for the ADMA charge transfer reaction as a function of solvent dielectric constant. The results allow us to apply Marcus theory to calculate the solvent-dependent activation energy for the charge transfer reaction of ADMA in the folded configuration. These results demonstrate that the reaction is not diffusion controlled in alkanes and are consistent with the theoretical results of Itoh and co-workers[20,21] and Ando,[17] which indicate that the barrier to electron transfer is of the same order of magnitude as the barrier to unfolding. The charge transfer rates measured in the most polar ethers studied in this paper are accelerated beyond the prediction of Marcus theory, and we use the results of section V to argue that this reflects a transition from the nonpolar to the polar mechanism. The central characteristic of this transition is that the reactant separation distance at which charge transfer occurs increases as the solvent dielectric constant increases across this solvent regime.

II. Methods

ADMA and APP (1-(9-anthryl)-3-phenylpropane), Figure 1, were synthesized according to the method outlined previously.[14,30] The solvents were obtained in the purest commercially available form, degassed with argon, and used without further purification. All measurements were made on 10^{-5} M samples thermostated at 25 °C.

The steady state fluorescence spectra were collected in a home-built scanning T-format fluorometer. The dispersed emission spectrum was collected with a photomultiplier tube through one arm, and the fluorescence at a fixed wavelength was collected synchronously and simultaneously through the other arm to correct for fluctuations in the emission intensity due to sample and instrumental conditions. The emission slit widths were set at 1.5 nm giving 3 nm resolution.

Time-correlated photon counting was performed by utilizing a mode-locked diode pumped Nd:YAG laser coupled to a dye laser. The dye laser was cavity dumped at 4 MHz. A β-BaB_2O_4 (BBO) crystal combined a 1064 nm IR beam with a 608 nm beam from the dye laser to obtain a 387 nm beam for excitation. The excitation beam was vertically polarized, and the emission was collected at the magic angle. The time-resolved emission wavelength was selected with a band-pass filter (10 nm fwhm) and was collected by a microchannel plate PMT (Hamamatsu, R 3809U-50). A typical instrument function has a 70 ps fwhm. The data were analyzed by the iterative reconvolution method using software of our own design that utilizes the Marquardt−Levenberg algorithm to minimize χ^2. ADMA equilibrium conformations were identified using semiempirical methods with Chem3D Pro (Cambridge Soft Corp.). Ab initio calculations of the model ions 9-methylanthracene and *p*-methyldimethylaniline were performed using Gaussian 2003[31] on the University of Missouri's Compaq AlphaServer Cluster.

TABLE 1: Solvent-Dependent Fluorescence Lifetimes of ADMA (τ) and APP (τ_0), and Calculated Charge Transfer Quenching Rate (τ_q)

solvent	τ_{ADMA} (ns)	τ_{APP} (ns)	τ_q[a] (ns)	η[b] (cP)	τ_q[c] (visc)(ns)	error[d] (%)
pentane	1.58	3.95	2.63	0.214	2.54	−3.4
hexane	1.73	4.29	2.90	0.297	2.94	1.5
heptane	2.00	4.31	3.73	0.391	3.33	−10.7
octane	2.20	4.89	4.04	0.513	3.77	−6.8
decane	2.66	5.47	5.17	0.841	4.71	−8.9
tetradecane	3.29	5.91	7.42	2.486	7.68	3.4
hexadecane	3.40	6.05	7.75	3.039	8.40	8.4
cyclopentane	2.05	4.86	3.55	0.423	3.45	−2.7
cyclohexane	2.48	5.85	4.30	0.905	4.87	13.2
cycloheptane	2.83	6.17	5.23	1.331	5.79	10.7
cyclooctane	3.37	6.95	6.54	2.260	7.35	12.4
dibutyl ether	2.16	6.39	3.26	0.646	4.18	28.2
dipropyl ether	1.32	4.36	1.89	0.402	3.37	78.6
tert-butylmethyl ether	0.61	4.97	0.695	0.340	3.13	350.2
diethyl ether	0.385	4.10	0.425	0.224	2.59	509.9

[a] Charge transfer quenching rates are calculated using eq 1. [b] Viscosities, η (cP), are taken from refs 53−58. [c] The quenching time predicted from the viscosity correlation calculated using eq *2*. [d] The error is calculated as a percent of the prediction based on eq 2. The RMS error for the alkanes is 8.5%.

III. Viscosity and Charge Transfer

Table 1 presents the experimentally determined fluorescence lifetimes collected at 420 nm for ADMA (τ), and APP (τ_0), dissolved in hydrocarbons and ethers. All radiative and nonradiative relaxation processes of APP with the exception of charge transfer are assumed to have the same rates as the analogous processes in ADMA. Experimental evidence from our lab has verified the validity of this assumption. For example, the fluorescence decays of APP and ADMA in mineral oil are shown in Figure 3. As the viscosity of the nonpolar solvent increases, the probability of charge transfer decreases, and at high enough viscosity the rate of charge transfer is expected to be insignificant. In mineral oil the decay times of APP and ADMA are very similar, indicating a small amount of charge transfer quenching. Similar results have been observed in glycerol.[32] Thus the rate of charge transfer quenching of the

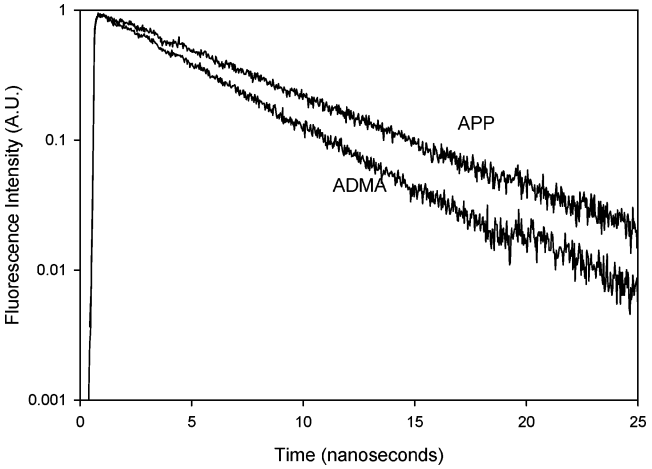

Figure 3. Fluorescence decays of the locally excited states of ADMA and APP in mineral oil at room temperature. The decays exhibit monoexponential behavior. The slight difference in the decay times is attributable to charge transfer quenching of the locally excited state of ADMA.

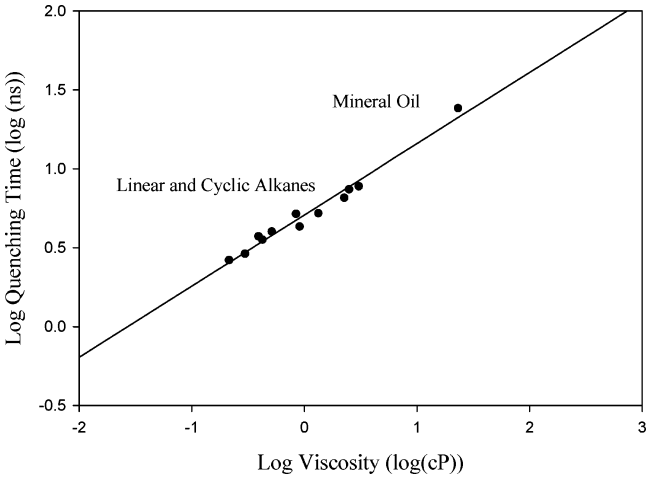

Figure 4. Logarithm of charge transfer quenching time of ADMA as a function of solvent logarithm of viscosity in alkanes and cyclic alkanes. The data are well represented by a viscosity power law (solid line) described in eq 3.

locally excited state emission in alkanes, $k_{alk} = (\tau_q(\text{alkane}))^{-1}$ can be determined using the relation[8,30]

$$\frac{1}{\tau_q} = \frac{1}{\tau} - \frac{1}{\tau_0} \tag{1}$$

Wang et al. refer to τ_q as the chain relaxation time. The calculated quenching rates for alkanes and ethers are given in Table 1. Wang et al.[8] have shown that the rate of charge transfer in ADMA exhibits a power-law dependence on viscosity (η, cP), τ_q (ns) $= 5.3\eta^{0.56}$, on the basis of measurements in isopentane, hexane, decane, and tetradecane. Figure 4 presents a plot of $\log(\tau_q)$ vs $\log(\eta)$ for a series of linear and cyclic hydrocarbon solvents, and the results correspond to the following power law,

$$\tau_q\,(\text{ns}) = 5.09\eta^{0.45} \tag{2}$$

which agrees well with the earlier work of Wang et al.[8] In fact, these two viscosity-dependent quenching rates are indistinguishable in the liquid alkane regime of viscosities. The data used to develop the correlation described by eq 2 spans 2 orders of magnitude in viscosity. Furthermore, measurements of quenching in glycerol and supercritical CO_2 indicate that this correlation is expected to be valid over 5 orders of magnitude in viscosity.

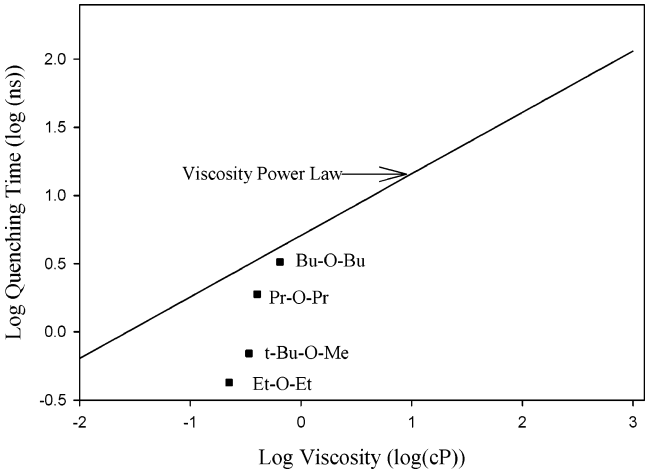

Figure 5. Logarithm of charge transfer quenching time of ADMA as a function of solvent logarithm of viscosity in ethers. The measured charge transfer quenching rates are accelerated over the rates predicted by the viscosity power law (solid line).

Figure 5 shows the fitted power law alongside measured charge transfer quenching rates of ADMA dissolved in four ethers, which have dielectric constants between 3 and 4.6. The diffusion controlled hypothesis predicts that the rate of charge transfer quenching of the locally excited state emission should depend only on solvent viscosity, as predicted by the power law in eq 2. However, Figure 5 indicates that in solvents of modest polarity the measured quenching rates deviate substantially from the power law derived from results in hydrocarbon solvents. The fluorescence decays of ADMA dissolved in ethers collected at 420 nm exhibit monoexponential kinetics, indicating that the nonpolar mechanism is operative. The accelerated rates observed in these solvents indicate that the nonpolar mechanism is not diffusion controlled in hydrocarbon solvents, and we take this as evidence that charge transfer is an activated process when the nonpolar mechanism is operative. The errors between the measured quenching rates and the quenching rates predicted from the viscosity power law correlation are presented in Table 1 for alkanes and ethers. The RMS error within the alkanes is 8.5%, and the errors of the ethers are 3−60 times this value. We postulate that the charge transfer reaction occurs along a trajectory that involves a folded intermediate, as shown in Figure 6, and we now describe the analysis of the quenching rate constant on the basis of this energy level scheme.

IV. Kinetic Analysis of the Nonpolar Mechanism

The kinetic scheme in Figure 6 depicts the extended LE state in equilibrium with the folded conformation of the LE state, and the equilibrium constant K_F is taken as the ratio of the folding (k_F) to unfolding (k_U) rates. On the basis of recent work by Itoh and co-workers[20,21] and Ando,[17] the barriers for "unfolding" and electron transfer are expected to be approximately 1 and 5 kJ/mol, respectively, the latter being characteristic of the barrier to electron transfer between the bimolecular reactants in acetonitrile at a distance of 5 Å. We apply the steady state approximation to the differential equation that describes the population of the folded conformation to solve the coupled differential equations that describe the populations of the LE, F and CT states of the molecule, as described in Figure 6. The decay of the LE state population can then be written as an uncoupled equation in the usual manner, with a

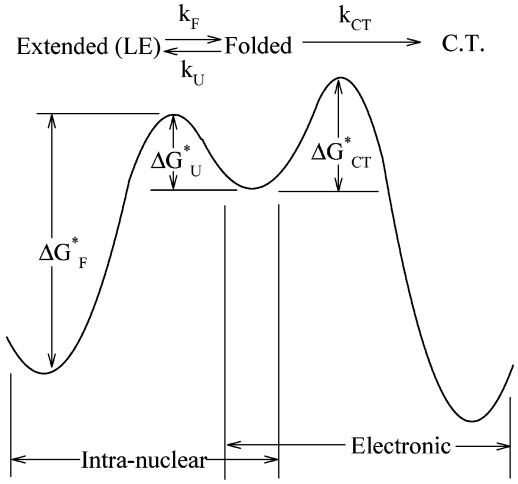

Figure 6. Schematic diagram of the postulated mechanism of ADMA charge transfer in nonpolar solvents. The barriers of electron transfer and "unfolding" are similar in magnitude.

rate constant that is the sum of the pathway shown in Figure 6 and the radiative and nonradiative relaxation rates exclusive of the pathway shown in Figure 6. Using eq 1 we arrive at an expression for the quenching rate due to charge transfer given by

$$k_q = \frac{K_F k_{CT}}{1 + \frac{k_{CT}}{k_U}} = \frac{k_F k_{CT}}{k_U + k_{CT}} \tag{3}$$

The first equality in eq 3 is analogous to the expression for bimolecular quenching in which K_F is the equilibrium constant for diffusive formation of the encounter complex, and k_U is the rate of diffusion of the reaction partners away from one another.[33] In analogy with the bimolecular expression, we expect the intramolecular quenching rate to be diffusion-limited when $k_{CT} \gg k_U$. Figure 5 suggests that this criterion is not met in ADMA dissolved in nonpolar solvents.

We will use the second form of eq 3 to derive an expression for the quenching rate that captures the essential features of the experimental results. The mechanism depicted in Figure 6 assumes that intramolecular motion may be required after the folding step in order for charge transfer to occur. In nonpolar liquids the solvent motion has a limited affect on the energy of the reactants, and we therefore expect intramolecular reorganization to have a relatively large influence on the rate at which the charge transfer barrier crossing occurs. For example, strong orbital overlap may be required for charge transfer in nonpolar solvents. In this case we would anticipate that vibration of the anthracene moiety against the dimethylaniline moiety would modulate the electronic state energies, and thereby assist the curve-crossing event. Because each elementary step may require solute nuclear motion, we model each frequency factor with a viscosity-dependent term as predicted for diffusive barrier crossing with friction by Kramers.[34] For example, the folding rate constant will have the form

$$k_F = \frac{A_F}{\eta^a} \exp\left(-\frac{\Delta G_F^*}{RT}\right) \tag{4}$$

where η is the bulk solvent viscosity. The exponent of the viscosity term is expected to be 1 on the basis of Kramers theory,[34] but in many cases it is found experimentally to be less than one.[35−45] Frequency-dependent friction near the top of the barrier is often invoked to explain the fractional exponent, which is thought to reflect the sharpness of the barrier, a sharper barrier leading to a smaller exponent.[46]

Expressions similar to eq 4 will be used for the unfolding reaction (with A_U, ΔG_U^* and η^γ) and the charge transfer reaction (with A_{CT}, ΔG_{CT}^*, and η^β). The frictional coupling of each specific type of solute intramolecular motion to the solvent is characterized by the viscosity exponents assigned to each elementary step in the mechanism. Substitution of these rate constants into eq 3 gives the following expression for the charge transfer quenching rate constant.

$$k_q = \frac{1}{\eta^\alpha} \frac{A_F \exp(-\Delta G_F^*/RT)}{\eta^{\beta-\gamma}\frac{A_U}{A_{CT}} \exp(-\Delta G_U^*/RT) \exp(\Delta G_{CT}^*/RT) + 1} \tag{5}$$

We can simplify this expression with the assumption that the barriers to folding and unfolding are insensitive to solvent, particularly in solvents of modest polarity. This assumption can be justified because these barriers are dominated by steric influences associated with conformational isomerization, which should not be sensitive to small changes in solvent properties. With these assumptions we arrive at a simple expression for the quenching time,

$$\tau_q = \eta^\alpha \left[\frac{1}{A_1} + \frac{A_2 \eta^{\beta-\gamma}}{A_1} \exp(\Delta G_{CT}^*/RT)\right] \tag{6}$$

where $A_1 = A_F \exp(-\Delta G_F^*/RT)$ and $A_2 = A_U/A_{CT} \exp(-\Delta G_U^*/RT)$ are constants at constant temperature. If ΔG_{CT}^* is constant and $\beta - \gamma$ is small, then eq 6 predicts that τ_q will exhibit a power law dependence on viscosity. If $\beta - \gamma$ is small, then the experimentally observed viscosity exponent primarily reflects the extent of frequency-dependent friction in the folding reaction. We can rationalize the postulate that $\beta - \gamma = 0$ with the argument that, in the folded geometry, the small amplitude motions required to achieve suitable orbital overlap for charge transfer will be similar to the small amplitude motions required to overcome a rotational barrier in the early part of the unfolding process, but we have not devised a method to test this assumption.

Though this model includes a number of simplifying assumptions, it captures two features of the anticipated solvent dependence of the ADMA quenching rate. First it predicts that within a series of solvents having similar activation barriers, the quenching time will follow a power law dependence on viscosity. Second, it predicts that for solvents of similar viscosity but different polarity, the quenching rate will be accelerated if the solvent polarity reduces ΔG_{CT}^*. In the case of ADMA the driving force for electron transfer is correlated with the solvatochromic shift of the charge transfer emission, and Figure 7 demonstrates that a plot of the natural log of the ratio of the quenching time in an ether to the quenching time predicted by the viscosity power law is approximately linear in the difference between the emission maxima of ADMA in the ether versus an alkane of similar viscosity. This result is anticipated on the basis of eq 6 under the assumption that $\beta - \gamma = 0$, and suggests that Marcus theory may be applicable to ADMA charge transfer in nonpolar solvents. In the following sections we calculate the free energy of electron transfer in ADMA by two methods. First we calculate the free energy directly from the energy of the ADMA 0−0 band absorbance and electrochemical data using the Rehm−Weller equation and solvent-dependent models for

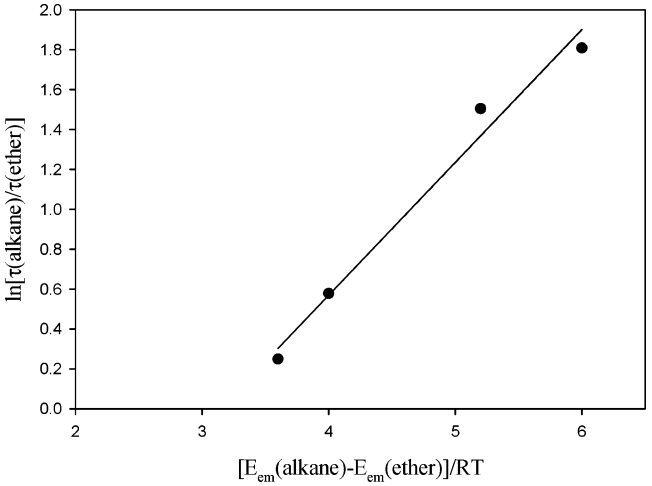

Figure 7. Comparison of the ratio of the charge transfer quenching times measured in ethers and alkanes of similar viscosity. The natural log of the ratios is correlated with the solvatochromic shift of the exciplex emission, which is consistent with the predictions of Marcus theory.

the work term and the solvation energy of the product ions. With these results we are also able to calculate the reorganization energy for ADMA electron transfer in acetonitrile. Second, we utilize the reorganization energy found from the first method and the energy of the 0−0 band absorbance to calculate the solvent-dependent free energy from emission spectral shifts. The latter results are used along with a model for the solvent reorganization energy to calculate the solvent-dependent activation energy of electron transfer in ADMA.

V. Application of the Rehm−Weller Model

The solvent dependence of ΔG^{ϵ}_{CT} for photoinitiated charge transfer reactions can be estimated from the Rehm−Weller expression,

$$\Delta G^{\epsilon}_{CT} = e\Delta E^{\epsilon} + w^{\epsilon} - E_{00} \qquad (7)$$

using spectroscopic and electrochemical data.[22] The solvent dependence of the parameters in eq 7 is made explicit by the superscript ϵ, which refers to the dielectric constant of the solvent. $e\Delta E^{\epsilon}$ is the electron charge (e) multiplied by the difference between the ground state oxidation potential of the electron donor and the ground state reduction potential of the acceptor (ΔE^{ϵ}). The oxidation potential of dimethylaniline in acetonitrile has a value of 0.78 V,[22] the reduction potential of anthracene in acetonitrile has a value of −2.07 V,[47] and $e\Delta E^{\epsilon}$ is 275 kJ/mol. E_{00} is determined from the measured absorption spectrum to be 309 kJ/mol (387 nm) and is independent of solvent. w^{ϵ} is the work required to bring the reactants to the separation distance at which charge transfer occurs. For bimolecular charge transfer reactions this is usually calculated as the Coulomb energy between two equal and opposite point charges separated by a specified distance in a medium of dielectric constant ϵ. (In this paper we assume that the charge transferred is equal to the charge of one electron.) The solvent dependence of the work term is the dielectric constant dependence of the Coulomb energy, and the solvent dependence of $e\Delta E^{\epsilon}$ is the dielectric constant dependence of the ion solvation energies.

When the donor and acceptor reactants are tethered, two issues must be addressed to properly account for the influence of the restricted reactant geometry on w^{ϵ}: (1) the need to account for the excess steric energy of preparing the excited reactants in proper juxtaposition for charge transfer and (2) the influence of hindered geometry on the calculation of the Coulomb energy. In addition, we must calculate the solvent-dependent ion solvation energies to estimate ΔG^{ϵ}_{CT} using eq 7. Before proceeding with the calculation of the solvent-dependent driving force for ADMA charge transfer, we digress to address these important issues.

Steric Effects. When donor and acceptor are tethered, the free energy of the charge transfer reaction is altered by the energy required to bring donor and acceptor into proper juxtaposition for charge transfer. Both donor and acceptor distance and relative orientation influence the coupling between locally excited and charge transfer states,[17] and therefore the rate of the charge transfer reaction. At any given conformation, if electronic coupling between the excited LE and CT states is weak, the accessible charge transfer pathway along the electronic coordinate will be nonadiabatic. In a flexible tethered donor−acceptor system such as ADMA, the relative orientation and distance of the donor and acceptor can change due to conformational isomerization during the course of the charge transfer reaction. Because nonadiabatic charge transfer is often much slower than adiabatic charge transfer, the reactants in a flexible, tethered donor acceptor system have the opportunity to find an adiabatic pathway by assuming conformations that simultaneously allow strong electronic coupling and spontaneous charge transfer. However, this requirement may result in an increase in the steric energy of the molecule, and the magnitude of this excess steric energy must be considered in the calculation of the reaction free energy.

We have examined several ground state conformations of ADMA with semiempirical methods at the PM3 level, and the results are shown in Table 2. Four of these conformations are local minima. The extended, folded, and "Kinked 2" configurations correspond to the atom configurations for the LE, SH, and LH states, respectively, shown in Figure 2. The tightly folded conformation was constructed from the folded geometry by adjusting the tether dihedral angles such that the van der Waals surfaces of the anthracene and dimethylaniline moieties were in contact with one another with their ring planes nearly parallel and then allowing a single minimization step. The distance between the planes of the donor and acceptor ring systems is 3 Å in the tightly folded conformation. This conformation is useful as a means of estimating the conformation of the charge transfer state, in which Coulombic attraction and steric energy are expected to balance one another at the equilibrium geometry. We use the term steric burden to refer to the excess conformational energy (relative to the extended form) of the molecule in the orientation at which electron transfer occurs. The steric burden has been estimated for the PM3-minimized conformations using the "steric energy" parameter following a single point MM2 calculation, and by the heats of formation reported following the PM3 minimization. Both methods give similar energies for the equilibrium geometries. The dramatic difference between these measures for the tightly folded geometry may represent the contribution of a single strained bond angle in the heat of formation result, because this measurement has not been minimized. Thus we anticipate that the molecular mechanics estimate is closer to reality in the charge transfer state of this conformation.

The energies of the kinked geometries indicate that these rotational isomers of the extended conformation are accessible at room temperature and do not represent a significant steric burden. Our values for kinked conformers are about a factor of 2 lower than Itoh's conformer energies of APP at the AM1

TABLE 2: Relative Steric Energies for Four Conformational Isomers of ADMA[a]

	equilibrium structures				
	extended	kinked 1	kinked 2	equilibrium folded	tightly folded
dihedral angles (deg)					
(1) 1−2−3−4	180	176	76	−69	−73
(2) 5−1−2−3	180	−73	−178	111	53
(3) 6−5−1−2	96	100	93	54	−145
av ring separation distance	7.8	6.2	6.8	5.3	4.4
steric burden to folding (SE, kJ/mol)	0	−1	2	12	30
steric burden to folding (HoF, kJ/mol)	0	1	4	16	108

[a] Steric burden refers to steric energy in excess of that for the extended configuration. Steric energy (SE) is the result of a MM2 single point calculation for the specified geometry, and the heat of formation (HoF) is the result of a PM3 minimization. The tightly folded geometry HoF is a single point calculation. All other values are local minima of ground state configurations. Dihedral angles (1)−(3) are defined with respect to the carbon index numbers given in the table. These refer to the numbering scheme given in Figure 1. Kinked 1 is a 120° rotation around bond 1−2. Kinked 2 is a 120° rotation around bond 2−3. Steric burden is measured relative to the steric energy and heat of formation of the extended form, whose values are 932 and 286 kJ/mol, respectively. The average ring separation distance is the arithmetic average of the pairwise atom distances between the donor and acceptor ring systems.

level.[20,21] The steric burden of the equilibrium folded conformation, on the other hand, is 10−20 kJ/mol and represents a substantial barrier to folding. Rotation around the 1−2 bond and rotation around the 2−3 bond are energetically feasible, and the rotational barriers are estimated from molecular mechanics and ethane rotational barriers to be on the order of 3 kJ/mol. But the resulting configurations retain the nearly orthogonal orientation of the donor and acceptor aromatic rings in the extended conformation. Because of the nearly orthogonal aromatic ring geometries, the extent to which these interconversions favor charge transfer will result primarily from changes in donor−acceptor distance, which is also estimated for the representative conformations in Table 2. The folded geometry results from substantial changes in all three dihedral angles given in the table, and supports a nearly face-to-face geometry with an aniline-anthracene ring face angle of about 30°. In the tightly folded geometry the aromatic rings are parallel, and substantial orbital overlap between donor and acceptor may occur. Vibrational motion of the aromatic ring systems toward and away from one another probably modulates the electronic coupling between the excited LE and CT states and may also represent motion along the reaction coordinate toward the curve crossing region. Thus this conformation may present an electronically adiabatic charge transfer pathway. The kinked geometry with additional rotation of the aniline ring may also result in increased donor−acceptor coupling, but the steric burden of the conformation with parallel aromatic rings exceeds 15 kJ/mol, owing to the close proximity of the ring hydrogens when the two aromatic ring systems are parallel to one another. These results characterize the steric burden required to attain a suitable geometry for charge transfer in ADMA. From the results shown in Table 2, a reasonable estimate of the steric burden of conformations for which strong coupling is expected in nonpolar solvents is 12 ± 2 kJ/mol.

Calculation of the Coulomb Energy. The second issue in estimating the work required to bring the reactants to the charge transfer geometry is the influence of conformational restrictions on the Coulomb energy. Coulomb energies for bimolecular photoinitiated electron transfer are calculated as

$$-q^2/(4\pi\epsilon_0\epsilon R_{sep}) \qquad (8)$$

where q is the electron charge, ϵ is the solvent dielectric constant, and R_{sep} is the distance that separates the reactants at the distance of charge transfer. Implicit in this form is the assumption that the reactants behave as point charges with respect to the energy gained via charge transfer. When the reactants are free to rotate about the molecular centers of mass, this expression may be adequate, because molecular rotation will modulate the interatomic distances, resulting approximately in a center of mass average separation distance. However, in tethered donor−acceptor systems, the reactant geometries are limited to a restricted set of conformational isomers. Thus the Coulomb energy is more properly considered as the sum of the Coulomb energies for a set of distributed charges.

We have use the following procedure to calculate the Coulomb energy for the distributed charges of the ADMA charge transfer state in the extended, folded, and tightly folded geometries. We begin with the Cartesian coordinates for these geometries described in Table 2 that are generated in the semiempirical calculation at the PM3 level. To assign charges to each atom position, we have performed ab initio calculations on 9-methylanthracene anion and *p*-methyldimethylaniline cation at the 6-31+G(d) level. We then map the Mulliken charges of all atoms in these ions onto the appropriate atoms of ADMA. One methyl hydrogen on each ion is eliminated in preparing the ADMA charge transfer complex from the ions, and the charge on this hydrogen is added to the methyl carbon from which it is removed. The center carbon of the propyl chain and its two hydrogen atoms are assumed to have zero charge, and this atom divides the anion charge distribution from the cation charge distribution. The model assumes that an accurate Coulomb energy can be calculated at a given neutral ADMA conformation by assigning charges from the model ions to the atoms of ADMA. (The advantage of this model is that it does not require ab initio calculation of ADMA excited states, though ultimately the validity of this approach must be tested by comparison with the full ab initio treatment of the ADMA molecule.) The Coulomb energy is calculated with a program of our own design, which calculates the sum of unique pairwise Coulomb energies between donor atoms and acceptor atoms. Coulomb energies thus calculated can be compared directly with the energies calculated in the point charge approximation described by eq 8.

The results of these calculations are given in Table 3. The tabulated values are in a vacuum, and values in various solvents can be calculated by simply dividing these values by the solvent dielectric constant. The Coulomb energy of an electron and a proton separated by 3 Å in a vacuum is −463 kJ/mol, whereas the Coulomb energy for ADMA in the tightly folded geometry (the separation of the parallel planes of the donor and acceptor aromatic rings is 3 Å) is −204 kJ/mol. We have performed this calculation with other lower level basis sets and find that the Coulomb energy ranges from −200 to −275 kJ/mol, which

TABLE 3: Coulomb Energies for a Model ADMA Charge Transfer System[a]

	extended	folded	tightly folded
Coulomb energy in a vacuum (kJ/mol)	−133.61	−184.7	−204.07

[a] The Cartesian coordinates of the charge system are taken from the semiempirical calculations of the ADMA conformations. Charges of the atoms of ADMA are generated by ab initio calculation of the methylanthracene anion and *p*-methyldimethylaniline cation at the 6-31+G(d) level. The center propyl carbon and its two hydrogen atoms are assumed to have zero charge.

corresponds to a charge separation distance ranging from 7 to 5 Å in the point charge approximation. Thus distributing the charge has the effect of reducing the Coulomb energy, which can be characterized by an increase in the "effective charge separation distance" in the point charge approximation described by eq 8.

This model does not account for charge redistribution due to intramolecular polarization nor have we identified the most favorable tightly folded configuration. Therefore we take the above results for the tightly folded geometry as the upper (i.e., most positive) limit to the Coulomb energy of the folded CT state, and the energy calculated for point charges separated by 3 Å is taken as the lower limit. Effective charge separation distances in the range 3−5 Å for the folded configuration conform to the limits of Coulomb energies described above. Coulomb energies calculated for the charge transfer state of the extended conformation are less sensitive to basis set effects and are characterized by effective charge separation distances from 7 to 10 Å in the point charge approximation. At the end of section V we will use experimental observations to refine our best estimates of the effective charge separation distance of the folded and extended conformations.

Ion Solvation. The term $e\Delta E^{\epsilon}$ in eq 7 depends on solvent, because the measured electrochemical potentials include the effect of ion solvation. To compute solvent-dependent values of ΔG^{ϵ}_{CT} using the Rehm−Weller expression, the ion solvation energies must be calculated for each solvent of interest. We will use the Born model for the ion solvation energy,

$$E_{solv} = -\frac{1}{8\pi\epsilon_0}\left(1-\frac{1}{\epsilon}\right)\left(\frac{q^2}{\rho}\right) \qquad (9)$$

which has been shown to be appropriate for solvation of aromatic ions.[48] q is the ion charge, ρ is the cavity radius of the ion, and ϵ is the dielectric constant of the solvent. We arrive at a systematic choice of ρ by the following procedure. The structures determined from the ab initio calculations of anthracene anion and dimethylaniline cation are use to calculate the solvent excluded volumes of the ions, which result in ionic radii of 3.39 and 3.00 Å, respectively, assuming spherical ions. We then compare the oxidation potential of dimethylaniline (E_{ox}) with its ionization potential (IP), and the reduction potential of anthracene (E_{red}) with its electron affinity (EA). Weller[49] has argued that $IP - E_{ox} = K - E_{solv,D}$, and $EA - E_{red} = K + E_{solv,A}$, where K is a constant equal to the difference between the vacuum level and the energy level of the electrochemical reference in the system used to measure the redox potentials. Anthracene's electron affinity is 51.1 kJ/mol, and dimethylaniline's ionization potential is 687 kJ/mol. Using these values, the redox potentials given at the beginning of section V, and the Born solvation energies calculated using the radii of the model ions, K is found to be 4.67 and 4.01 eV for anthracene and dimethylaniline, respectively. We postulate that the difference in the value of the constant thus determined results from improper choice of the cavity radii, and we use Weller's relation[49] to estimate effective radii for the anthracene and dimethylaniline ions by requiring

$$EA - IP = E_{red} - E_{ox} + (E_{solv,A} + E_{solv,D}) \qquad (10)$$

Solvation energies are calculated for acceptor ($E_{solv,A}$) and donor ($E_{solv,D}$) using eq 9, and the ion radii are systematically adjusted until eq 10 is satisfied. The adjusted radii for the anion and cation are 3.98 and 3.53 Å, respectively. These values result in a reference potential energy of 4.36 eV, which is close to the approximate value of ∼4.7 eV that has been estimated for the standard hydrogen electrode.[50] Calculated free energies of electron transfer are insensitive to small variations in the ionic radii used for these calculations. For example, if the anion radius is increased by 5% and the cation radius is decreased by 5%, the anion and cation solvation energies will change, but the total solvation energy of the system will not change.

Calculation of the Free Energy of Electron Transfer. We wish to calculate ΔG^{ϵ}_{CT} as a function of solvent dielectric constant via eq 7 for both extended and folded conformations of the ADMA CT state. The above discussion highlights the following facts. (1) The work term must include the steric burden of the folded CT state, whereas the extended state is assumed to have no additional steric burden. (2) The Coulomb energy must be calculated as a function of dielectric constant of the solvent. (3) The effective charge separation distance used in the calculation of the Coulomb energy will be in the range 3−5 Å for the folded form and 7−10 Å for the extended form. This accounts for the influence of distributed charge on the Coulomb energy. (4) The driving force given by eq 7 includes the influence of ion solvation in acetonitrile through the $e\Delta E$ term. Therefore ion solvation energies must be corrected for solvent dielectric constant to estimate the dependence of the driving force on dielectric constant. We use the following expression to calculate the driving force.

$$\Delta G^{\epsilon}_{CT} = e\Delta E^{37.5} - E^{37.5}_{solv,A} - E^{37.5}_{solv,D} + E^{\epsilon}_{solv,A} + E^{\epsilon}_{solv,D} + E_{steric}(r) + E_{Coulomb}(r) - E_{00} \qquad (11)$$

This is a form of eq 7 in which the steric and Coulomb terms are given explicitly, the solvation energies of the ions in the solvent in which redox potentials were measured (i.e., acetonitrile) have been subtracted, and the solvation energies of the ions in the solvent of dielectric constant ϵ have been added. Solvation energies of ADMA are calculated as the sum of the solvation energies of the anthracene and dimethylaniline ions in a solvent of dielectric constant ϵ using eq 9 for both the extended and folded forms. A steric energy of $E_{steric}(r) = 12$ kJ/mol is added to the driving force for the folded form. Coulomb energies are calculated for several effective separation distances using eq 8. The values of ΔG^{ϵ}_{CT} thus calculated are shown in Table 4 for a range of solvent dielectric constants and effective charge separation distances of 4 Å (folded) and 8 Å (extended).

Next we examine the sensitivity of ΔG^{ϵ}_{CT} to choice of effective charge separation distance used in the Coulomb energy term. Figure 8 is a plot of driving force versus solvent dielectric constant calculated for effective charge separation distances ($R_{sep,folded}$) of 3−5 Å for the folded conformation, and effective charge separation distances ($R_{sep,extended}$) of 7−9 Å for the extended conformation. The extended results vary somewhat at low dielectric constants but are essentially identical for

TABLE 4: Solvent Dielectric Constant (ϵ) Dependence of the Driving Force to Charge Transfer in Extended and Folded Conformations[a]

			extended		folded		
ϵ	$E_{solv,A}$	$E_{solv,D}$	$E_{Coulomb,E}$	$\Delta G_{ct,E}$	$E_{Coulomb,F}$	$\Delta G_{ct,F}$	folded fraction
1	0.00	0.00	−173.67	154.18	−347.34	−7.50	100%
2	−91.37	−94.37	−86.84	55.28	−173.67	−19.56	100%
3	−121.82	−125.82	−57.89	22.31	−115.78	−23.58	100%
4	−137.05	−141.55	−43.42	5.83	−86.84	−25.59	100%
5	−146.19	−150.98	−34.73	−4.06	−69.47	−26.79	100%
6	−152.28	−157.28	−28.95	−10.65	−57.89	−27.60	100%
10	−164.46	−169.86	−17.37	−23.84	−34.73	−29.21	100%
12	−167.51	−173.00	−14.47	−27.14	−28.95	−29.61	100%
14	−169.68	−175.25	−12.41	−29.49	−24.81	−29.90	100%
15	−170.55	−176.15	−11.58	−30.43	−23.16	−30.01	84%
16	−171.31	−176.94	−10.85	−31.26	−21.71	−30.11	63%
18	−172.58	−178.25	−9.65	−32.63	−19.30	−30.28	39%
20	−173.60	−179.29	−8.68	−33.73	−17.37	−30.41	26%
25	−175.43	−181.18	−6.95	−35.71	−13.89	−30.65	13%
30	−176.64	−182.44	−5.79	−37.02	−11.58	−30.81	8%
35	−177.51	−183.34	−4.96	−37.97	−9.92	−30.93	6%
37	−177.80	−183.63	−4.69	−38.27	−9.39	−30.97	5%
38	−177.93	−183.76	−4.57	−38.41	−9.14	−30.98	5%
40	−178.17	−184.01	−4.34	−38.67	−8.68	−31.02	5%

[a] Driving force is calculated by eq 7. Solvation energies are calculated by eq 9. Coulomb energies for extended and folded conformations are calculated with effective charge separation distances of 8 and 4 Å, respectively. The steric energy of 12 kJ/mol is added to the free energy of the folded conformation for all values of ϵ.

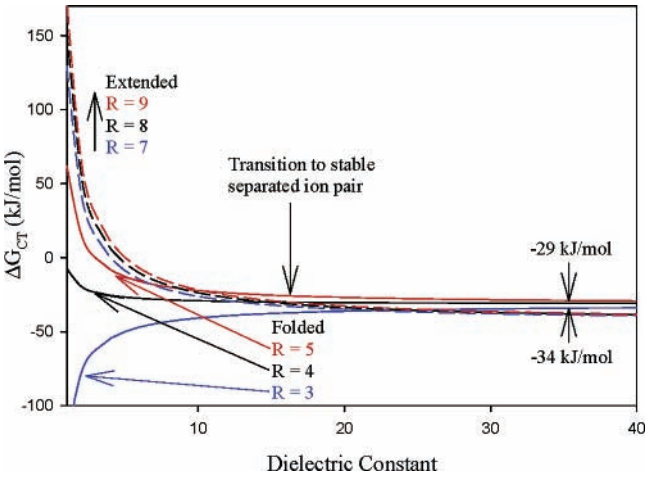

Figure 8. Dependence of free energy of electron transfer on solvent dielectric constant for the extended and folded conformations. Dashed lines are for the extended conformation. Solid lines are for the folded conformation. Plots for three different values of the effective charge separation distance, *R*, are given. The extended results are practically independent of *R* for dielectric constants greater than 15. The variation with *R* for the folded results at the dielectric constant of acetonitrile are shown in the plot. The extended conformation of the charge transfer state becomes stable at a dielectric constant of about 16, where the Coulomb energy of the extended form crosses to a more negative value than the folded form.

dielectric constants greater than 15. The extended conformation of the charge transfer state has a positive free energy until ϵ is greater than 4 or 5, though the value at which ΔG^{ϵ}_{CT} turns negative is weakly dependent on the choice of $R_{sep,extended}$. Note, however, that the results are independent of *R* when $\epsilon = 37.5$. The free energies of charge transfer in the folded conformation show larger sensitivity to $R_{sep,folded}$ across the entire range of dielectric constants, but experimental results allow us to refine our estimate of this parameter. In a vacuum an effective separation greater than 4 results in positive free energies. Syage, Felker, and Zewail[51] have demonstrated that ADMA undergoes charge transfer under isolated jet conditions, which supports the choice of 4 Å as an upper limit to $R_{sep,folded}$, because this is the largest separation that results in a negative free energy in a vacuum.[52] Moreover, they estimate the thermodynamic stabilization of the exciplex in a vacuum to be −38 kJ/mol, and this value corresponds to an effective charge separation distance of ∼3.7 Å in our model. It is also interesting to note that the activation barrier estimated from the vibronic energy dependence of the exciplex emission in the jet-cooled ADMA is 11 kJ/mol, which compares favorably with our estimate of a 12 kJ/mol steric burden for the folding reaction. An effective charge separation of 3 Å results in a free energy in a vacuum that exceeds −100 kJ/mol, which seems unrealistically large. Based on these comparisons, our best estimates of the effective separation distances are $R_{sep,folded} = 4$ Å and $R_{sep,extended} = 8$ Å. The numerical results based on these values are shown in Table 4 and are consistent with experimental studies of ADMA charge transfer kinetics, as discussed in the following paragraph.

The values of ΔG^{ϵ}_{CT} in Table 4 for the extended conformation indicate that the charge transfer reaction becomes spontaneous in this conformation between dielectric constant values of 4 and 5. This is consistent with the well-known transition from the nonpolar to polar mechanism, as illustrated in Figure 2. Previous studies in our lab have demonstrated that this transition is experimentally observable as a change from single exponential to double exponential decay of the anthracene emission at a dielectric constant of 5. The mechanism depicted in Figure 2 indicates that the resulting extended charge transfer state favors the folded conformation, which is also consistent with the results shown in Table 4, for although the extended CT reaction is spontaneous above a dielectric constant of 5, the folded conformation is thermodynamically favored. This ultimately results in a folded charge transfer conformation, even when the charge transfer event occurs in the extended form. Because the folded conformation is emissive, the presence of the folded form in polar solvents can be monitored via fluorescence measurements. For example, charge transfer emission is particularly strong in tetrahydrofuran, a solvent in which the charge transfer reaction is known to proceed via the polar mechanism. The folded form is favored until the free energy of the extended form is lower than the free energy of the folded form. According to Table 4, this occurs at a dielectric constant of about 15, at which point the extended ↔ folded equilibrium supports 16% of the molecules in the nonemissive extended form. This is also consistent with the observed diminution of charge transfer emission in solvents having dielectric constants greater than 20.[7] In these solvents, little charge transfer emission is observed, owing to the solvent stabilization of the charge-separated conformation of the ADMA CT state. This reflects the fact that the Coulomb stabilization does not compensate for the steric burden of folding in highly polar solvents due to increased screening as the dielectric constant is increased. In acetonitrile, electronically excited ADMA exists almost exclusively in the charge-separated form when the two forms are in equilibrium, which is reflected in the absence of emission from ADMA in this solvent. Thus it appears that the effective charge separation distances of 4 and 8 Å for the folded and extended conformations, respectively, along with a steric burden of ∼12 kJ/mol are consistent with the observed dependence of the charge transfer mechanism on solvent.

VI. Application of Marcus Theory

Marcus theory predicts that the activation energy for charge transfer is related to the free energy change, ΔG^{ϵ}_{CT}, and to the

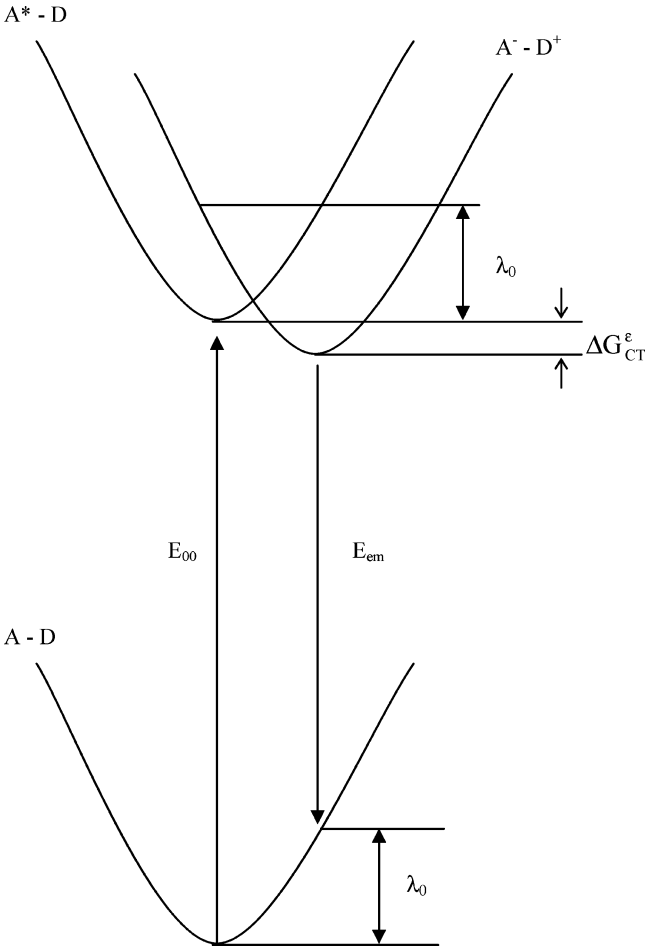

Figure 9. Potential energy scheme for analysis of the charge transfer barrier height.

total reorganization energy λ_0^ϵ via

$$\Delta G^*_{CT} = \frac{\lambda_0^\epsilon}{4}\left(1 + \frac{\Delta G^\epsilon_{CT}}{\lambda_0^\epsilon}\right)^2 \tag{12}$$

The total reorganization energy, λ_0, includes contributions from intramolecular coordinates, which are assumed to be solvent independent, as well as solvent coordinates. Figure 9 gives a schematic representation of the potential energy surfaces pertinent to this analysis. In this description, we assume that the parabolas representing the three participating electronic states have the same force constants. In addition, we assume that the ground state surface and the LE surface have same equilibrium position along the reaction coordinate. This assumption is justified, because the ground state and the locally excited state have similar solvent response, as indicated by the small solvatochromic shifts of the ADMA locally excited state spectra. Under these assumptions, the reorganization energy in the excited state is the same as the reorganization energy that characterizes the Franck−Condon configuration of the ground state following exciplex emission. From Figure 9 the thermodynamic driving force for the reaction can be expressed as

$$\Delta G^\epsilon_{CT} \cong E^\epsilon_{em} - E_{00} + \lambda_0^\epsilon \tag{13}$$

Thus the Stokes Shift between the absorption and exciplex emission spectra characterizes the sum of the Gibbs free energy for the charge transfer reaction plus the reorganization energy.

We can utilize eqs 12 and 13 to calculate the barrier to charge transfer in the following manner. First we utilize the Gibbs free energy of the ADMA charge transfer reaction in acetonitrile calculated from eq 7 as described in section V. Using this value, the known value of the photon absorption energy, and the value of the emission energy in acetonitrile determined from solvatochromic studies,[14] we can determine the reorganization energy for the reaction in acetonitrile. We then utilize measured absorption and emission energies along with the solvent-corrected reorganization energies calculated using the continuum model of Brunschwig, Ehrenson, and Sutin[53] to determine the Gibbs free energy of reaction in the ethers. Finally, these results along with the solvent-corrected reorganization energies are used to calculate the activation barrier in ethers using eq 12. Each of these steps is described in more detail below.

Total Reorganization Energy in Acetonitrile. For the purpose of calculating the reorganization energy in acetonitrile, the most significant feature of Figure 8 is the fact that the free energies of charge transfer in the folded conformation only vary by ±10% as the effective charge separation distance varies. From Table 4, our best estimate of the free energy of charge transfer in acetonitrile in the folded conformation is -31 ± 3 kJ/mol, where the uncertainty is the geometric sum of the uncertainties of the free energy estimate and the steric burden. We use this value in eq 13 to estimate the reorganization energy of the ADMA charge transfer reaction in acetonitrile. E_{em} for the exciplex in acetonitrile is estimated to be 222 kJ/mol (540 nm) from our previously published solvatochromic study[14] using the equation

$$E_{em}\,(\text{kJ/mol}) = -51.1[F] + 262 \tag{14}$$

where

$$F = \frac{2(\epsilon - 1)}{2\epsilon + 1} - \frac{n^2 - 1}{2n^2 + 1} \tag{15}$$

E_{00} is taken as 309 kJ/mol in all solvents. Using these values in eq 13, λ_0 is estimated to be 56 kJ/mol, and this along with the free energy of charge transfer gives an activation energy of 2.8 kJ/mol when used in eq 12.

Solvent Reorganization Energy. The total reorganization energy is the sum of the solvent reorganization energy λ_s^ϵ and the internal reorganization energy λ_v. The value of λ_v can be considered to be solvent independent.[54] Brunschwig, Ehrenson, and Sutin[53] have shown that the solvent-dependent term of the reorganization energy is given by

$$\lambda_s^\epsilon = \frac{{\mu_e}^2}{4\pi\epsilon_0 a^3}\frac{3(\epsilon - n^2)}{4(\epsilon + 2)(n^2 + 2)} \tag{16}$$

in the dielectric continuum approximation for a polarizable point dipole, where ϵ_0 is the permittivity of vacuum, a is the radius of a spherical cavity having the same volume as the solute molecule, and μ_e is the dipole moment of the exciplex.[55] Using eq 16, the solvent-dependent contribution to the reorganization energy for the ADMA charge transfer reaction in acetonitrile is 18.2 kJ/mol, and therefore the intramolecular contribution to the reorganization energy is 37.8 kJ/mol.

It is instructive to compare these results for λ_s and λ_v with the results of Cosa and Chesta[26] and with the results of Gould et al.[56,57] Cosa and Chesta devised a method of extracting λ_v for bimolecular CT complexes from CT emission peak shifts that is independent of the value of λ_s. They demonstrated that

TABLE 5: Calculated Driving Force and Barrier Height for the ADMA Charge Transfer Reaction in the Folded Conformation

solvent	ϵ^a	n^a	λ_s^ϵ (kJ/mol)	E_{em} (kJ/mol)	ΔG_{CT}^ϵ (kJ/mol)	$\Delta G_{CT}^{\neq}$ (kJ/mol)
pentane	1.84	1.375	−0.26	253	−18.3	2.47
hexane	1.89	1.375	0.00	252	−18.7	2.41
heptane	1.93	1.388	0.02	252	−19.0	2.35
octane	1.95	1.397	−0.01	252	−19.1	2.31
decane	1.99	1.410	0.01	252	−19.4	2.25
tetradecane	2.04	1.429	−0.01	252	−19.7	2.18
hexadecane	2.06	1.435	0.00	251	−19.8	2.15
cyclopentane	1.97	1.407	−0.05	252	−19.2	2.28
cyclohexane	2.02	1.427	−0.08	252	−19.5	2.20
cycloheptane	2.08	1.444	−0.02	251	−19.9	2.12
cyclooctane	2.13	1.459	0.01	251	−20.2	2.06
dibutyl ether	3.08	1.399	4.28	242	−24.7	1.81
dipropyl ether	3.38	1.381	5.37	240	−25.5	1.80
tert-butylmethyl ether	4	1.369	7.01	237	−26.8	1.80
diethyl ether	4.26	1.353	7.77	236	−27.3	1.83
acetonitrile	37.5	1.344	18.20	222	−31.2	2.76

[a] Dielectric constants and refractive indices taken from ref 59.

their measured values are consistent with semiempirical calculations based geometric differences between neutral and ionic forms of the donors and acceptors. For complexes of dimethylaniline and polycyclic aromatic acceptors, their average measured value is $\lambda_v = 40$ kJ/mol, in excellent agreement with our calculations using $\lambda_s = 18$ kJ/mol. For complexes of arene donors and dicyanoarene acceptors, Cosa and Chesta measure $\lambda_v = 20$ kJ/mol, in excellent agreement with the results of Gould et al., who studied bimolecular systems of cyanoanthracenes and alkylbenzenes. But whereas the values of λ_v appear to agree across experiments, the values for λ_s show significant variations. Our calculated value for the solvent reorganization energy of ADMA in acetonitrile ($\lambda_s = 18$ kJ/mol) is smaller than that calculated by Cosa and Chesta for the triethylamine−methylnaphthalene bimolecular complex in acetonitrile ($\lambda_s = 28$ kJ/mol). This discrepancy arises because we use a model that includes solute polarizability appropriate for a tethered, flexible intramolecular CT complex, whereas Cosa and Chesta use a model that does not include solute polarizability.[53] Our value of λ_s and Cosa and Chesta's value of λ_s are significantly smaller than values typical of the results of Gould et al. ($\lambda_s \sim 50$ kJ/mol) for di- and tetracyanoanthracene acceptors and alkylbenzene donors. Gould et al. determine λ_s by fitting CT emission spectra to a golden rule-type model of emission intensity. They also note that these systems form ground state complexes. The discrepancy between λ_s for ADMA and λ_s for cyanoanthracene−alkylbenzene systems may be related to differences in electron distributions within these systems, and they may be related to the differences in methods used to determine the solvent reorganization energies. Nevertheless, our value of $\lambda_s = 18$ kJ/mol in acetonitrile generates a set of results that are consistent across all models used in this paper.

Calculation of the Electron Transfer Activation Energy. Because the intramolecular contribution to the reorganization energy is solvent independent, we use the value of λ_v determined in acetonitrile for all subsequent calculations. Equation 16 is used to determine λ^ϵ_s, eqs 14 and 15 give the solvent-dependent emission energy, and these parameters are used in eqs 12 and 13 to determine the solvent-dependent barrier to electron transfer in ADMA. The results of this calculation are shown in Table 5. The free energies for the charge transfer reaction in the folded conformation in Table 4 calculated using the Rehm−Weller expression are in excellent agreement with the values in Table 5 calculated on the basis of eq 13. The activation energies for electron transfer in the folded conformation shown in Table 5 are calculated from the solvent-dependent values of λ^ϵ_s and ΔG^ϵ_{CT} using eq 12. The results indicate that the barrier to electron transfer decreases in ethers compared to alkanes. They also demonstrate that electron transfer in the folded configuration of ADMA in acetonitrile is in the Marcus inverted regime. This is consistent with Ando's[17] simulations, which predicts a decrease in the electron transfer rate of ADMA in acetonitrile at separation distances less than 4 Å.

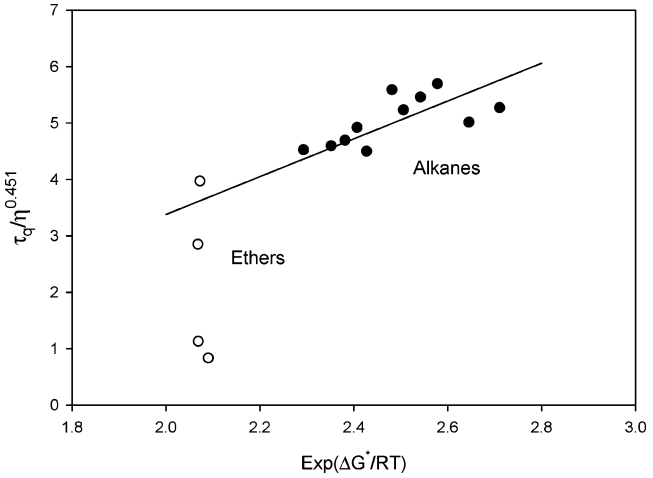

Figure 10. Analysis of measured quenching times and viscosities according to eq 6. The equation predicts a linear correlation between the ratio of quenching time to viscosity and the exponential term in the rate law governing charge transfer in ADMA. Filled circles are alkane results and open circles are ethers.

VII. Discussion

The results shown in Table 5 are consistent with the assumptions used in developing the simple model of activated charge transfer in ADMA. The barrier height in alkanes is relatively constant, though a systematic trend toward lower barrier is apparent as the chain length is increased, and in the transition to cyclic alkanes. This is not unexpected, because cyclic alkanes can have small dipole moments by virtue of nonsymmetric conformations. The fact that the calculated barrier height in alkanes is approximately equal to the bond rotational barrier associated with unfolding indicates that the criterion for diffusion control of the charge transfer reaction is not met in the flexible, tethered ADMA system.

Though the calculated free energies of charge transfer exhibits significant differences between alkanes and ethers, the effect is more subtle in the barrier height. The former effect is also apparent in the solvatochromism of the ADMA exciplex emission. An increase in solvent polarity results in a more pronounced difference between the reactant and product energies. However, the influence of the driving force on the barrier to charge transfer is mitigated by the concomitant solvent dependence of the reorganization energy.

The activation barriers in Table 5 are based on Marcus theory. If the rate acceleration in ethers is the result of product stabilization, and if eq 6 adequately represents the rate constant for charge transfer quenching, then a plot of τ_q/η^α vs exp ($\Delta G^*/RT$) should be linear with a positive slope when the calculated activation barriers are used. Figure 10 presents such a plot in which α, the exponent determined from the viscosity power law correlation, has a value of 0.45. The parameters used to calculate the values along the *y*-axis are determined experimentally, whereas the data along the *x*-axis are determined from the

analysis summarized in Table 5. The plot exhibits a linear correlation over most of the data. Thus acceleration of the charge transfer rate appears to result from product stabilization and is consistent with Marcus theory.

The two most polar ethers in Figure 10 exhibit quenching rates that are accelerated beyond the prediction of the linear correlation. These solvents have dielectric constants of 4 and 4.3, which places them in the solvent regime where a transition from nonpolar-to-polar mechanism is expected on the basis of Table 4 and Figure 8. Three effects can accelerate the electron transfer rate of ADMA in this regime. First, the solvent can stabilize the folded CT state of ADMA, thereby accelerating electron transfer according to the Marcus expression, eq 12. Second, orientational motion of the polar solvent can alter the trajectory of the system along the reaction coordinate, and thereby increase the probability of electron transfer per unit time. Third, the polar solvent can stabilize the kinked and extended conformations of the CT state, and thereby increase the distance at which electron transfer is thermodynamically possible. The latter effect should be observable as a biexponential decay of the LE state fluorescence. Experimentally, the ethers exhibit single exponential fluorescence decays from the LE state. Kinetic analysis of the polar mechanism indicates that the ratio of the amplitudes of the fast and slow decay components depends on the ratio of the forward to reverse charge transfer rate constants. When the solvent dielectric constant is in the range of 4.5, the driving force for forward charge transfer in the extended conformation is small, and the ratio of forward to reverse electron transfer rate constants may be close to unity. This may prevent observation of biexponential character in the fluorescence decay, particularly if the decay constants are similar in magnitude. Still, the rapidly increasing rate of electron transfer in this regime appears to reflect a transition from nonpolar to polar mechanism, as predicted in Table 4 and Figure 8.

The analysis that leads to Figure 8 indicates that stabilization due to solvation results in spontaneous electron transfer at a dielectric constant of 5 in the extended conformation. However, the transition to the thermodynamically favored extended conformation at a dielectric constant of 15 occurs because dielectric screening diminishes the Coulombic stabilization of the folded form so much that it is no longer able to overcome the steric burden of the folded conformation.

Our picture of the ADMA charge transfer reaction is that of the reactants searching conformation space for an adiabatic charge transfer pathway. In polar solvents, this view is corroborated by Ando's simulations.[17] In nonpolar solvents, folding is required, first to find a conformation at which charge transfer is spontaneous, and second to find a geometry in which electronic coupling is strong. Orientational restrictions and the absence of polar solvent molecules may diminish electronic coupling in some conformations, whereas certain intramolecular modes may result in substantial coupling in a configuration that supports spontaneous charge transfer. We note that, although Ando's simulations indicate that the bimolecular charge transfer reaction is in the inverted regime in acetonitrile at separation distances less than 4 Å, in ADMA the inverted regime will not be observed, because the adiabatic charge transfer reaction will occur in the extended conformation before the molecule isomerizes to a conformation with the appropriate reactant separation. Finally, recent measurements in our lab indicate that solvent relaxation governs the rate of electron transfer in the polar mechanism, and this is consistent with strongly coupled, adiabatic electron transfer in extended conformations. This result will be the subject of another paper.

Acknowledgment. We thank the referees for their careful review of this manuscript. This research was supported in part by the National Science Foundation (NSF-CHE-9508744) and the University of Missouri Research Board.

References and Notes

(1) *The Exciplex*; Gordon, M., Ware, W. R., Eds.; Academic Press: New York, 1975; p 372.
(2) Hui, M.-H.; Ware, W. R. *J. Am. Chem. Soc.* **1976**, *98*, 4718.
(3) Okada, T.; Fujita, T.; Kubota, M.; Masaki, S.; Mataga, N.; Ide, R.; Sakata, Y.; Misumi, S. *Chem. Phys. Lett.* **1972**, *14*, 563.
(4) Masaki, S.; Okada, T.; Mataga, N.; Sakata, Y.; Misumi, S. *Bull. Chem. Soc. Jpn.* **1976**, *44*, 1277.
(5) Migita, M.; Okada, T.; Mataga, N.; Nakashima, N.; Yoshihara, K.; Sakata, Y.; Misumi, S. *Chem. Phys. Lett.* **1980**, *72*, 229.
(6) Chuang, T. J.; Cox, R. J.; Eisenthal, K. B. *J. Am. Chem. Soc.* **1974**, *96*, 6828.
(7) Crawford, M. K.; Wang, Y.; Eisenthal, K. B. *Chem. Phys. Lett.* **1981**, *79*, 529.
(8) Wang, Y.; Crawford, M. C.; Eisenthal, K. B. *J. Am. Chem. Soc.* **1982**, *104*, 5874.
(9) Wang, Y.; Crawford, M. K.; Eisenthal, K. B. *J. Phys. Chem.* **1980**, *84*, 2696.
(10) Okada, T.; Migita, M.; Mataga, N.; Sakata, Y.; Misumi, S. *J. Am. Chem. Soc.* **1981**, *103*, 4715.
(11) Khajehpour, M.; Welch, C. M.; Kleiner, K. A.; Kauffman, J. F. *J. Phys. Chem. A* **2001**, *105*, 5372.
(12) Khajehpour, M.; Kauffman, J. F. *J. Phys. Chem. A* **2001**, *105*, 10316.
(13) Khajehpour, M.; Kauffman, J. F. *J. Phys. Chem. A* **2000**, *104*, 9512.
(14) Khajehpour, M.; Kauffman, J. F. *J. Phys. Chem. A* **2000**, *104*, 7151.
(15) We have determined experimentally that the polar mechanism is operative when the solvent dielectric constant is greater than 5 by pure and mixed solvent studies.
(16) Kavarnos, G. J. *Fundamentals of Photoinduced Electron transfer*; VCH: New York, 1993.
(17) Ando, K. *J. Chem. Phys.* **1994**, *101*, 2850.
(18) Kumar, K.; Kurnikova, I. V.; Beratan, D. N.; Waldeck, D. H.; Zimmt, M. B. *J. Phys. Chem. A* **1998**, *102*, 5529.
(19) Kumar, K.; Lin, Z.; Waldeck, D. H.; Zimmt, M. B. *J. Am. Chem. Soc.* **1996**, *118*, 243.
(20) Takasu, R.; Kizu, N.; Itoh, M.; Shinoda, H. *J. Chem. Phys.* **1994**, *101*, 7364.
(21) Kizu, N.; Itoh, M. *J. Am. Chem. Soc.* **1993**, *115*, 4799.
(22) Rehm, D.; Weller, A. *Isr. J. Chem.* **1979**, *8*, 259.
(23) Barbara, P. F.; Meyer, T. J.; Ratner, M. A. *J. Phys. Chem.* **1996**, *100*, 13148.
(24) Costa, S. M. d. B.; Prieto, M. J. *J. Photochem.* **1983**, *23*, 343.
(25) Hirsch, T.; Port, H.; Wolf, H. C.; Miehlich, B.; Effenberger, F. *J. Phys. Chem. B* **1997**, *101*, 4525.
(26) Cosa, G.; Chesta, C. A. *J. Phys. Chem. A* **1997**, *101*, 4922.
(27) Kapturkiewicz, A.; Nowacki, J. *J. Phys. Chem. A* **1999**, *103*, 8145.
(28) Chesta, C. A.; Avila, V.; Soltermann, A. T.; Previtali, C. M.; Cosa, J. J.; Crystall, B.; Phillips, D. *J. Chem. Soc., Faraday Trans.* **1996**, *92*, 3327.
(29) Burgdorff, C.; Loehmannsroeben, H.-G.; Sander, T. *J. Chem. Soc., Faraday Trans.* **1996**, *92*, 3043.
(30) Khajehpour, M.; Kauffman, J. F. *Chem. Phys. Lett.* **1998**, *297*, 141.
(31) Frisch, M. J.; Trucks, G. W.; Schlegel, H. B.; Scuseria, G. E.; Robb, M. A.; Cheeseman, J. R.; Montgomery, J. A., Jr.; Vreven, T.; Kudin, K. N.; Burant, J. C.; Millam, J. M.; Iyengar, S. S.; Tomasi, J.; Barone, V.; Mennucci, B.; Cossi, M.; Scalmani, G.; Rega, N.; Petersson, G. A.; Nakatsuji, H.; Hada, M.; Ehara, M.; Toyota, K.; Fukuda, R.; Hasegawa, J.; Ishida, M.; Nakajima, T.; Honda, Y.; Kitao, O.; Nakai, H.; Klene, M.; Li, X.; Knox, J. E.; Hratchian, H. P.; Cross, J. B.; Adamo, C.; Jaramillo, J.; Gomperts, R.; Stratmann, R. E.; Yazyev, O.; Austin, A. J.; Cammi, R.; Pomelli, C.; Ochterski, J. W.; Ayala, P. Y.; Morokuma, K.; Voth, G. A.; Salvador, P.; Dannenberg, J. J.; Zakrzewski, V. G.; Dapprich, S.; Daniels, A. D.; Strain, M. C.; Farkas, O.; Malick, D. K.; Rabuck, A. D.; Raghavachari, K.; Foresman, J. B.; Ortiz, J. V.; Cui, Q.; Baboul, A. G.; Clifford, S.; Cioslowski, J.; Stefanov, B. B.; Liu, G.; Liashenko, A.; Piskorz, P.; Komaromi, I.; Martin, R. L.; Fox, D. J.; Keith, T.; Al-Laham, M. A.; Peng, C. Y.; Nanayakkara, A.; Challacombe, M.; Gill, P. M. W.; Johnson, B.; Chen, W.; Wong, M. W.; Gonzalez, C.; Pople, J. A. *Gaussian03*, revision B.04; Gaussian, Inc.: Pittsburgh, PA, 2003.
(32) Glycerol is highly polar, and therefore the polar mechanism is operative. We have demonstrated that charge transfer in the polar rate is governed by solvent relaxation, and does not occur in glycerol at room temperature. In glycerol the decays of APP and ADMA are identical. These results will be presented in a separate publication.
(33) Kavarnos, G. J. *Top. Curr. Chem.* **1990**, *156*, 21.

(34) Kramers, H. A. *Physica* **1940**, *7*, 284.
(35) Rettig, W.; Fritz, R.; Braun, D. *J. Phys. Chem. A* **1997**, *101*, 6830.
(36) Velsko, S. P.; Waldeck, D. H.; Fleming, G. R. *J. Chem. Phys.* **1983**, *78*, 249.
(37) Jaeger, W.; Schneider, S.; Verhoeven, J. W. *Chem. Phys. Lett.* **1997**, *270*, 50.
(38) Nadler, W.; Marcus, R. A. *J. Chem. Phys.* **1987**, *86*, 3906.
(39) Calef, D. F.; Wolynes, P. G. *J. Phys. Chem.* **1983**, *87*, 3387.
(40) Bulgarevich, D. S.; Kajimoto, O.; Hara, K. *J. Phys. Chem.* **1995**, *99*, 13356.
(41) Kometani, N.; Kajimoto, O.; Hara, K. *J. Phys. Chem. A* **1997**, *101*, 4916.
(42) Heitele, H.; Michel-Beyerle, M. E.; Finckh, P. *Chem. Phys. Lett.* **1987**, *138*, 237.
(43) Hara, K.; Akimoto, S.; Suzuki, H. *Chem. Phys. Lett.* **1990**, *175*, 493.
(44) Bagchi, B.; Oxtoby, D. W. *J. Chem. Phys.* **1983**, *78*, 2735.
(45) Berezhkovskii, A. M.; Zitserman, V. Y.; Lin, S. H. *J. Chem. Phys.* **1997**, *107*, 10539.
(46) Bagchi, B. *Int. Rev. Phys. Chem.* **1987**, *6*, 1.
(47) Kubota, T.; Miyazaki, H.; Ezum, K.; Yamakawa, M. *Bull. Chem. Soc. Jpn.* **1974**, *47*, 491.
(48) Katoh, R.; Lacmann, K.; Schmidt, W. F. *J. Electron Spectrosc.* **1996**, *78*, 419.
(49) Weller, A. *Z. Phys. Chem.* **1982**, *133*, 93.
(50) Morrison, S. R. *The Chemical Physics of Surfaces*, 2nd ed.; Plenum: New York, 1990.
(51) Syage, J. A.; Felker, P. M.; Zewail, A. H. *J. Chem. Phys.* **1984**, *81*, 2233.
(52) The effective charge separation distance of 4 Å used in the calculation of the Coulomb energy is less than the sum of the ionic radii used to calculate the solvent-dependent solvation energy of the solute. This discrepancy arises because the spherical cavity approximation is used in the Born model of ion solvation. The separation between the planes of the aromatic donor and acceptor rings in the folded conformation as determined by semiempirical structure optimization is 3 Å. The effective charge separation distance is expected to be larger than the physical separation, because the effect of distributed charge on the calculated Coulomb energy is characterized by an increase in the effective charge separation distance when the point charge approximation is used.
(53) Brunschwig, B. S.; Ehrenson, S.; Sutin, N. *J. Phys. Chem.* **1987**, *91*, 4714.
(54) Sutin, N. *Prog. Inorg. Chem.y* **1983**, *30*, 441.
(55) Abell, G. C.; Funabashi, K. *J. Chem. Phys.* **1973**, *58*, 1079.
(56) Gould, I. R.; Young, R. H.; Moody, R. E.; Farid, S. *J. Phys. Chem.* **1991**, *95*, 2068.
(57) Gould, I. R.; Farid, S. *J. Phys. Chem.* **1992**, *96*, 7635.